

New Gasoline and Gas Barrier from Plasticized Carbon Black Reinforced Butyl Rubber/High-Density Polyethylene Blends

Farid El-Tantawy,¹ Nadia Abdel Aal²

¹Department of Physics, Faculty of Science, Suez Canal University, Ismailia, Egypt

²Chemistry Department, Faculty of Science, Suez Canal University, Ismailia, Egypt

Received 14 January 2005; accepted 29 March 2005

DOI 10.1002/app.22742

Published online 14 April 2006 in Wiley InterScience (www.interscience.wiley.com).

ABSTRACT: The effects of the high-density polyethylene volume fraction on the curing characteristics and network structure of rubber blends have been studied in terms of the torque, scorch time, optimum curing time, Mooney viscosity, number of elastically effective chains, viscosity, interfacial tension, glass-transition temperature, scanning electron microscopy, internal friction, sound velocity, acoustic attenuation, polymer-solvent interaction parameter, swelling index, and gel fraction. The applicability of the blends for gasoline barriers has been examined through the changes in the electrical resistance and volumetric swelling in gasoline versus time at room temperature. The transport mechanism of the solvent through the crosslinked butyl rubber/high-density polyethylene blends is governed by Fickian diffusion law. The transport coefficients, namely, the diffusion coefficient, intrinsic diffusion, and permeation coefficient, have been computed. The experimental data for the permeation coefficient are in good agreement with the values calculated by Maxwell's model and far from those of Robeson's model. In addition, some thermodynamics parameters,

namely, the standard entropy, standard enthalpy, and standard Gibbs free energy, have been estimated as functions of the high-density polyethylene concentration of the butyl rubber blends. Furthermore, the applicability of butyl rubber/high-density polyethylene composites for Freon gas barriers and antistatic charge dissipation has been examined. Finally, the mechanical properties, such as the tensile strength, hardness, stiffness, and elongation at break, of butyl rubber composites with different high-density polyethylene concentrations have been evaluated. The increase in the mechanical properties is due to the increase in the crosslinking density and the interfacial adhesion of the blend. This proves that these new blends have important technological applications as gasoline and Freon barriers and for antistatic charge dissipation with good mechanical properties. © 2006 Wiley Periodicals, Inc. *J Appl Polym Sci* 101: 1237–1247, 2006

Key words: blends; gas permeation; mechanical properties; networks; swelling

INTRODUCTION

The concept of physically combining two or more polymers via blending to obtain new polymeric materials with desired properties has received a lot of attention because of both fundamental and practical interest.^{1,2} The phenomenon of blending can be implemented more rapidly and economically. This technique has helped to develop many new materials that are of good quality and are cheaper on the market. The properties of a blend depend mainly on the continuous phase, but factors such as the amount, size, shape, and interfacial adhesion of the dispersed phase also play a role.^{3,4} However, conducting polymer blends are used in a wide variety of industrial applications such as battery and full-cell electrodes, antistatic media, and corrosion-resistant materials.^{5–7} In fact, domestic and environmental applications need the de-

velopment of barrier solvents and gases to prevent pollution. Conducting thermoplastic-elastomer blends seem to be very promising in this respect because of their low cost of production, simple method of preparation, and good stability.^{8,9} The swelling properties of polymers are mainly related to the elasticity of the network, the extent of crosslinking, and the porosity of the polymer.^{10,11} The determination of the resistance of a polymer to solvents and gases is standardized in test procedures before the polymer finds successful applications involving exposure to such solvents and gases.^{12,13} Laminated molding hose composed of an inner tube of polyamide and an outer tube of butyl rubber (IIR) has been proposed to enhance the gas-resistance properties, but it shows insufficient flexibility because of interfacial segregation.⁹ Freon gas has been used as a refrigerant in air-conditioning systems, and its use is now severely restricted because of its ability to destroy the ozone layer and its greenhouse-effect potential.^{14,15} To solve this problem and associated complexity, the gas resistance and absorption of the vibration of the compressor in air-conditioning systems of rubber hose must be improved. As one of

Correspondence to: F. El-Tantawy (faridtantawy@yahoo.com).

TABLE I
Basic Formulation Used for IIR/HPE Blends^a

Ingredient	HPE0	HPE10	HPE20	HPE30	HPE40	HPE50
IIR	100	90	80	70	60	50
HPE	0	10	20	30	40	50
ZnO	3	3	3	3	3	3
CuCl ₂	2	2	2	2	2	2
Glycerol	10	10	10	10	10	10
CB	25	25	25	25	25	25
TMTD ^b	1	1	1	1	1	1
CBS ^c	1	1	1	1	1	1
Silane-602	1	1	1	1	1	1
Sulfur	1.5	1.5	1.5	1.5	1.5	1.5

^a The ingredients were arranged in the same way used during preparation.

^b Tetramethyl thiuram disulfide.

^c *N*-Cyclohexyl-2-benzothiazyl sulfenamide.

the ways of overcoming these problems, the use of IIR and high-density polyethylene (HPE) blends reinforced with plasticized carbon black (CB) has been suggested. Therefore, new conducting IIR/HPE blends, which resist the diffusion of gasoline and Freon gas and have good flexibility, have been fabricated. The effect of the HPE concentration on the cure characteristics and network structure of the blends has been investigated in detail. The applicability of the IIR/HPE blends for gasoline barriers has been tested through the monitoring of the changes in the electrical resistance and volumetric swelling (VS) with time during the swelling process. The diffusion mode of the blends has been studied. Some thermodynamics parameters such as the entropy (ΔS), enthalpy (ΔH), and Gibbs free energy (ΔG) of swollen samples have been estimated. Furthermore, the Freon gas barriers and static charge for IIR/HPE have been examined. Finally, the mechanical properties of IIR/HPE blends have been studied. These blends have important technological applications for gasoline and Freon shielding and antistatic charge dissipation materials with good mechanical properties.

EXPERIMENTAL

Materials and sample preparation

IIR in this study was a commercial grade (IIR-754) purchased from Alexandria Trade Rubber Co. (Alexandria, Egypt). HPE (trade name HPE-700) was supplied by Hillbillies Petrochemical Co. (Cairo, Egypt). Poly(*p*-phenylene) was used as a plasticizer and was purchased from Outsoka Chemical Co. (Tokyo, Japan). An amine triethoxysilane coupling agent (trade name Silane-KBM-602) was produced by Shin-Etsu Chemical Co., Ltd. (Tokyo, Japan). The formulations of the blends are given in Table I. The blends of IIR and HPE were prepared in ratios of 100/0, 90/10, 80/20, 70/30, 60/40, and 50/50 (wt %) and are desig-

nated HPE0, HPE10, HPE20, HPE30, HPE40, and HPE50, respectively, where the numbers indicate the weight percentages of HPE in the blends. The physical mixing of the blends was carried out with a two-roll mill at room temperature and at a rotor speed of 40 rpm. The curatives were added to the blend during the roll-mixing process according to the standard compounding procedures. The mixed compound was preheated for 10 min and cured for 30 min at 155°C under a pressure of 350 kN/m².

Characterization

The microstructure of the specimens was observed with a scanning electron microscopy (SEM) instrument (model 8650, JEOL, Tokyo, Japan) with an acceleration voltage of 30 kV. Carbon ink was painted on the surfaces of the samples to improve the surface conduction. The cure characteristics, such as the torque and optimum cure time (t_{90}), were determined with a Monsanto MDR 2000 moving die rheometer (New York) according to ASTM D 2240-93. The Mooney scorch time (S_t) was determined with a Monsanto MV 2000 automatic Mooney viscometer. S_t is defined as the time required for an increase of 4 units above the minimum viscosity, as determined from a plot of the Mooney viscosity versus time. The viscosity (η) was determined with a viscometer (VM-A, Kio, Tokyo, Japan). The interfacial tension (γ) of the blends was tested by contact-angle measurements with a CA-2000 (Asahi, Tokyo, Japan) contact-angle meter. The glass-transition temperature (T_g) and degree of crystallinity (DC) were determined by differential scanning calorimetry (DSC) with a Shimadzu DSC-60 apparatus. DC was determined with the following relation:⁴

$$DC = \frac{\Delta H_f}{\Delta H_f^0 W_f} \quad (1)$$

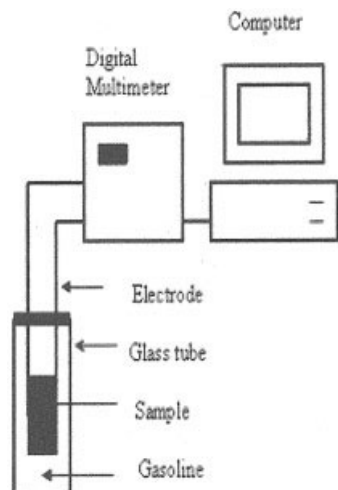


Figure 1 Apparatus for the measurement of electric resistance during swelling in gasoline at room temperature (20°C).

where ΔH_f is the apparent enthalpy of fusion (indicated in DSC thermograms as the melting enthalpy per gram of the blend) corresponding to the component, ΔH_f^0 is the enthalpy of fusion per gram of the component in its completely crystalline state, and W_f is the weight fraction of the component.

The internal friction (Q^{-1} or IF) was measured at 25°C with a multifunction IF apparatus in the force vibration mode at 1 kHz. The sound velocity (SV) and acoustic attenuation (AU) were measured with a Krautkramer–Branson USD-10 ultrasonic flaw detector. The adapted technique was the pulse–echo immersion technique. AU was calculated with the following relation:¹⁶

$$AU = \frac{20}{h} \log \left(\frac{U_s}{U_w \delta^2} \right) \quad (2)$$

where U_s and U_w are the amplitudes of the transmitted bursts measured with and without the sample, respectively, and δ is the transmission coefficient.

The equipment used to measure the electrical resistance during swelling in a solvent (gasoline) is schematically shown in Figure 1. For swelling studies, a known weight of a specimen was left to swell in toluene until no further increase in the weight of the specimen was observed. This was considered the equilibrium swelling weight of the specimen. The swollen specimen was vacuum-dried to a constant weight. The swelling index (SI) and gel fraction (GF) were calculated with simple mathematical relations:¹⁷

$$SI (\%) = \frac{A_s}{W_1} \times 100 \quad (3)$$

$$GF = \frac{W_2}{W_1} \quad (4)$$

where A_s is the amount of the solvent absorbed by the sample, W_1 is the initial weight of the blend sample before swelling, and W_2 is the weight of the dried sample.

VS was calculated with the following relation:^{4,18}

$$VS (\%) = \frac{(m_t - m_0)\rho_r}{\rho_s} \times 100 \quad (5)$$

where ρ_s and ρ_r are the solvent and polymer densities, respectively; m_t is the mass of the swollen polymer at time t ; and m_0 is the mass of the dry polymer at time 0.

The permeability of Freon gas through an IIR/HPE blend with a thickness of about 3 mm at room temperature was determined by gas chromatography. The static energy (SE) of the IIR/HPE blends was measured with a static charge meter (model AX-221, Tokyo, Japan) and calculated with the following relation:⁴

$$SE = \frac{1}{2} CV_m^2 \quad (6)$$

where C is the capacitance of the base plate and V_m is the voltage indicated on the static charge meter.

Dumbbell-shaped test specimens were cut from the dry vulcanized sheets. Mechanical testing of the samples was performed at 25°C according to the ASTM D 412-80 test method at a crosshead speed of 40 mm/min with a universal testing machine.

RESULTS AND DISCUSSION

Cure characteristics, interaction parameters, and chain density of the IIR/HPE blends

To understand the influence of HPE on the cure kinetics and processability of the IIR matrix, knowledge of various parameters, such as the torque, S_t , optimum curing time, and Mooney viscosity, is of vital importance. Figure 2(a) shows rheographs of the IIR/HPE blends. The torque initially decreases, then increases, and finally levels off. The initial decrease in the torque to a minimum value is due to the ordering of the networks and softening of the polymer matrix, whereas the increase in the torque is due to the crosslinking of the blends. The leveling-off of the torque is an indication of the completion of the curing reaction. The blend containing 50 wt % HPE has a maximum torque value indicating greater crosslinking and stiffness. This is due to the activation of an adjacent double bond by the HPE group that causes an overall increase in the rate of crosslinking of the blend.

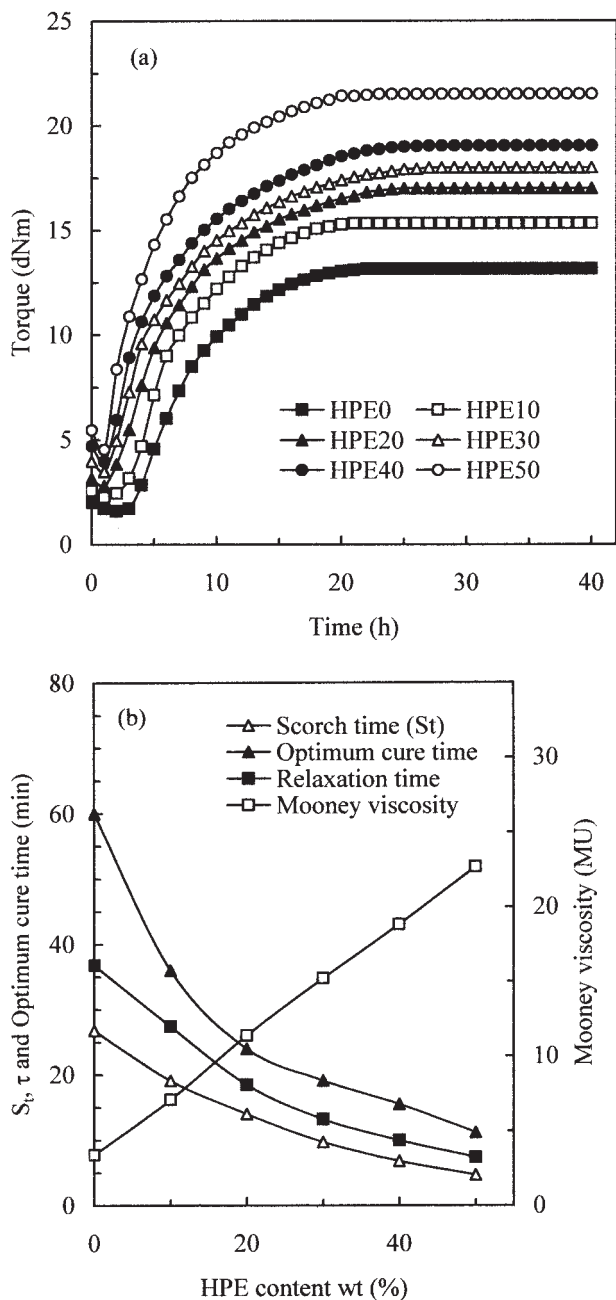


Figure 2 (a) Torque versus the time for IIR/HPE blends and (b) variation of S_t , τ , t_{90} , and the Mooney viscosity of IIR/HPE blends.

With increasing HPE concentration, more activated precursors to crosslink are formed as a result of the activation of the double bond by the HPE group. These activated precursors accelerate the vulcanization between the IIR and HPE phases and induce faster interphase crosslinking between these molecules.¹⁹

The torque–time curve of the blends during cure starting at the gel point can be expressed by the following empirical formula:

$$\frac{G_m - G(t)}{G_m - G_0} = \exp\left(-\frac{t}{\tau}\right) \quad (7)$$

where G_m and G_0 are the final and initial torque values during curing, respectively; $G(t)$ is the torque at time t ; and τ is the time parameter (relaxation time) of the reaction system and is calculated as $t = \tau$.

The dependence of τ , S_t , the optimum curing time, and the Mooney viscosity at 150°C on the HPE concentration is plotted in Figure 2(b). τ , S_t , and the optimum curing time decrease with increasing HPE loading in the blends. This is attributed to the increase in the adhesion force between HPE and the rubber matrix. This means that the addition of HPE accelerates the curing rate and the driving force of the curing reaction of the system. Also, the HPE50 sample shows lower t_{90} and S_t values than the other samples. This reflects the fact that the inclusion of HPE accelerates the curing kinetic reaction and increases the crosslinking density of the blend. The Mooney viscosity increases with increasing HPE loading. This fact indicates that the addition of HPE increases the interaction between HPE and the matrix and the stiffness of the blends, as confirmed before. However, the number of elastically effective chains (NEC) of a blend vulcanizate has been determined from swelling data with the Flory–Rehner equation.⁶ The average molecular weight between crosslinks (M_c) can be calculated with the following equation:^{4,20}

$$M_c = \frac{-V_1 \rho_r \left(V_r^{\frac{1}{3}} - \frac{V_r}{2} \right)}{[\ln(1 - V_r) + V_r + cV_r^2]} \quad (8)$$

where V_1 is the molar volume of the solvent and V_r is the volume fraction of the polymer in a swollen mass. V_r is given by

$$V_r = \frac{(d - f_w) \rho_r - 1}{(d - f_w) \rho_r - 1 + A_s \rho_s - 1} \quad (9)$$

where d is the deswollen weight of the specimen and f_w is the volume fraction of the insoluble components.

The blend–solvent interaction parameter (c) is given by^{7,8}

$$c = \frac{V_l (\gamma_s - \gamma_r)^2}{RT} \quad (10)$$

where γ_s and γ_r are the solubility parameters of the gasoline and blend, respectively; R is the universal gas constant; and T is the absolute temperature.

From M_c , NEC can be calculated with the following equation:

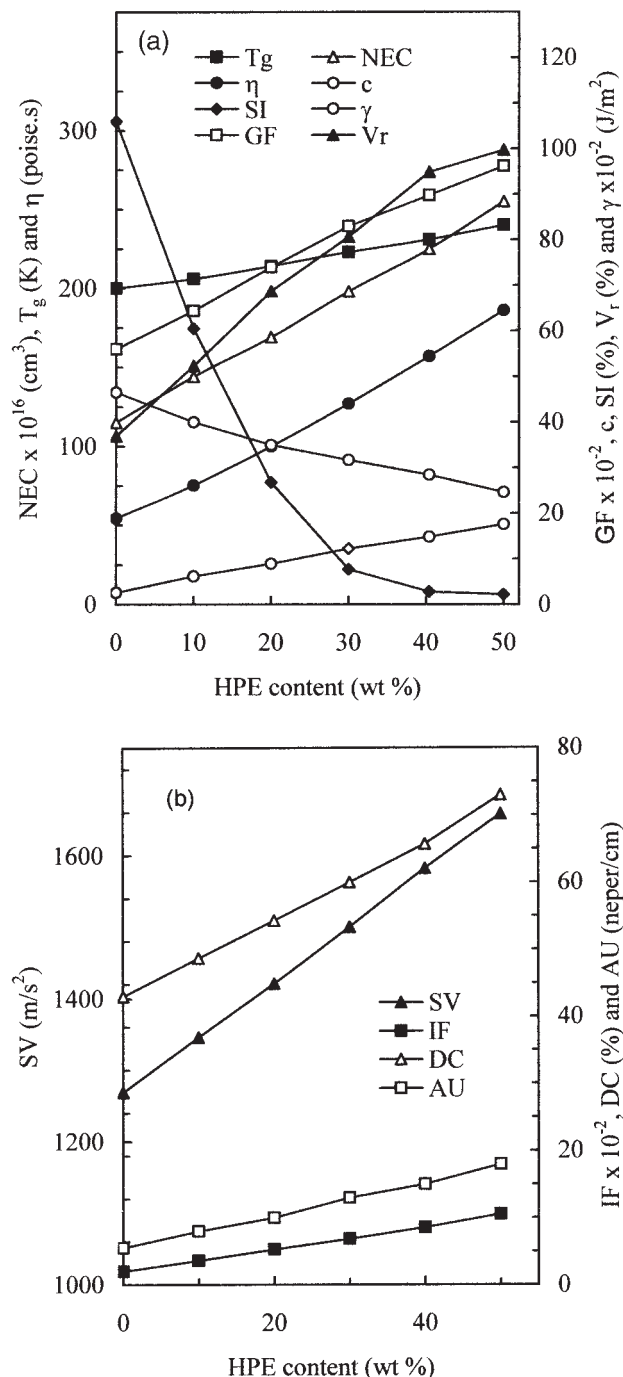


Figure 3 (a) Dependence of NEC, η , γ , T_g , c , GF, V_r , and SI on the HPE concentration for six different samples at room temperature and (b) variation of IF, SV, AU, and DC of IIR/HPE blends.

$$NEC = \frac{\rho_r N_A}{M_c} \quad (11)$$

where N_A is Avogadro's number.

The dependence of NEC, T_g , η , and c on the HPE concentration for six different samples at room temperatures is shown in Figure 3(a). NEC of the blend

increases with increasing HPE concentration. This indicates that the addition of HPE further reduces the void volume fraction and, therefore, increases the chain connectivity (i.e., increases the interaction between HPE and the rubber matrix). The higher NEC value noted for the HPE50 sample is due to higher chain entanglement and better molecular-level mixing. The T_g values increase with an increase in the HPE concentration, as shown in Figure 3(a). The presence of HPE in the IIR matrix leads to a shift in T_g to a higher temperature. This shows that HPE has a strong effect on the mobility segment of the rubber matrix and association between IIR and HPE in the blend. Furthermore, the observed enhancement in T_g is believed to be due to the restraint of the mobility of the rubber chains and the increase in DC of the blends with an increase in the HPE concentration in the blends, as shown in Figure 3(b).

However, the increase in η values with increasing HPE loadings indicates that as more and more HPE chains get into the rubber matrix, the mobility of the macromolecular chains of the rubber decreases, and this results in more rigid vulcanizates. Also, the γ values increase with increasing HPE concentration. This may be attributed to enhanced crosslinking of the matrix in the presence of HPE, which causes a further increase in the crosslinking density of the polymer matrix.¹⁹

Again, to analyze the interaction between the blend components of the system, the SI, c , and GF values versus HPE have been estimated, and the results are plotted in Figure 3(a). SI and c decrease with increasing HPE concentration. This can be ascribed to the increase in the crosslinking density and volume fraction of the polymer (V_r) with increasing HPE loadings, as shown in Figure 3(a). Sample HPE50 shows the minimum SI and c values, which indicate that HPE acts as a bonding agent to the rubber matrix, and so swelling is highly restricted in the blend. GF increases with increasing HPE concentration. This increase can be simply attributed to the inherent nature of the HPE used, as it tends to crosslink more quickly and a fibril-like structure may be inducing entanglements that contribute to a higher gel content.

Additional confirmatory evidence for the crosslinking density and interaction between the blend components of the system has been obtained by an analysis of SV, AU, and IF as functions of the HPE concentration, as shown in Figure 3(b). The increase in SV and IF of the blends with increasing HPE concentration is due to the fact that the segmental mobility of the blends might be reduced and therefore the intermolecular forces of the blend network structure and interfacial adhesion of the blends might be increased. We have observed that AU values increase with increasing HPE concentration in the blends. We propose that the increase in attenuation comes from the fact

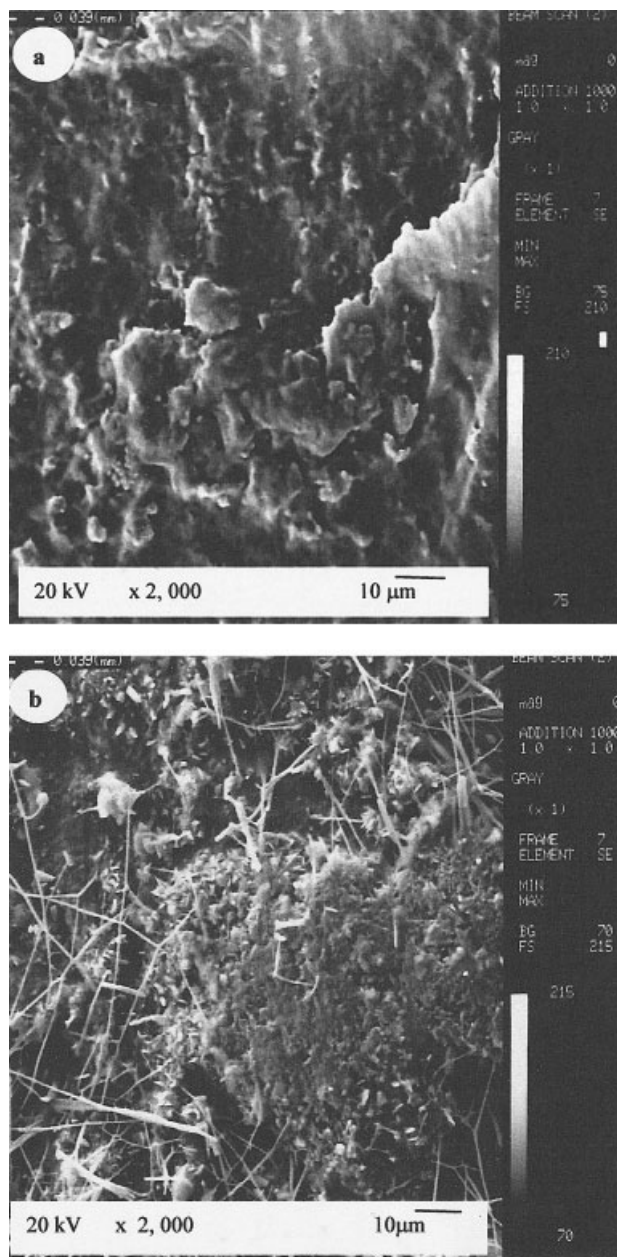


Figure 4 SEM micrographs of IIR/HPE blends (a) with an HPE loading of 0 wt % before swelling and (b) with an HPE loading of 50 wt % before swelling.

that the fibril-like structure of the blends precludes the wave-matter interaction and, therefore, the acoustic wave scatters into the blends.¹⁶

SEM

SEM micrographs of IIR/HPE blends with 0 and 50 wt % HPE are shown in Figure 4(a,b), respectively. A comparison of Figure 4(a,b) leads to the very interesting observation that the pores of HPE0 have decreased and the CB particles have good interactions with the rubber matrix. In HPE50, IIR is the continuous phase,

and the HPE particles are dispersed and are seen as fiber lines. The HPE fiber reacts with the IIR matrix, which serves as a crosslinking former. Also, sample HPE50 has a more homogeneous microstructure than HPE0. The microstructural homogeneity of the IIR/HPE blend may be attributed to the good dispersion and interfacial adhesion between HPE and the rubber matrix. Therefore, the homogeneous microstructure and good interfacial adhesion of the IIR/HPE blends may enhance the network links and, therefore, resist the diffusion of solvent/gas molecules within the blends, as confirmed previously and later in this article.

Applicability of the IIR/HPE blends as gasoline barriers

Figure 5(a) presents the dependence of the electrical resistance for IIR/HPE blends on the time of swelling in gasoline at 25°C. The electrical resistance of the blends strongly depends on the HPE concentration. At a low HPE concentration of less than 30 wt %, the electrical resistance increases with the swelling time and then levels off according to the HPE concentration. There are two reasons for the increase in the resistance with time. First, insulating clusters form from the gasoline molecules around the conductive particles. Second, the crosslinking density decreases, and the intermolecular distance between the conductive particles increase. This leads to the fast diffusion and transport of solvent molecules and degrades the chain filaments within the polymer blends. With the HPE concentration increasing beyond 30 wt %, there is no significant change in the resistance of the IIR blends.

These results are also confirmed by the activation energy (E_a) values for unswollen and swollen samples in Figure 5(b) calculated with the following relation:¹⁸

$$\rho = \rho_0 e^{-E_a/K_B T} \quad (12)$$

where ρ_0 is the initial conductivity and K_B is the Boltzmann constant.

E_a of the blend increases with an increase in the HPE concentration. The marked differences observed in E_a for unswollen and swollen samples may be due to the degradation effect of the swollen molecules in the blend matrix. At a low HPE concentration of less than 30 wt %, the segmental mobility of the blend may be increased by the diffusion of gasoline molecules and, therefore, may weaken the intermolecular bonds of the blend network structure. Therefore, the conductive phases are built up and segregate at the grain boundaries within the polymer matrix, and there is no conductive filament of the network formed; this leads to the increase in the resistance.⁴

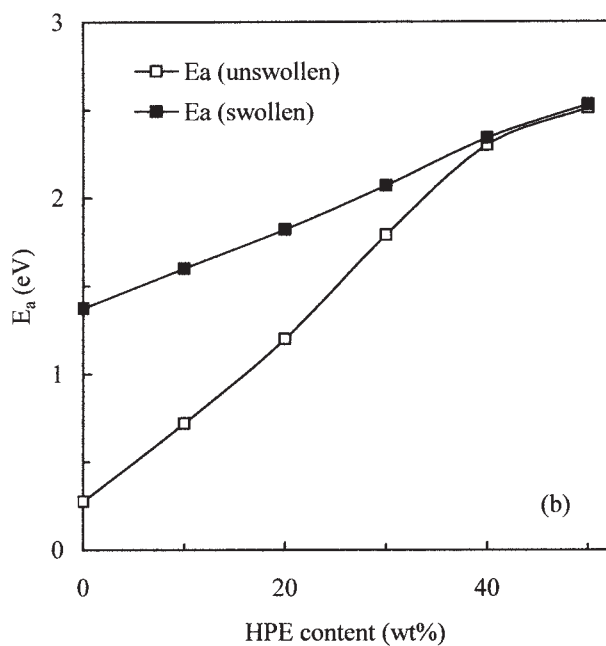
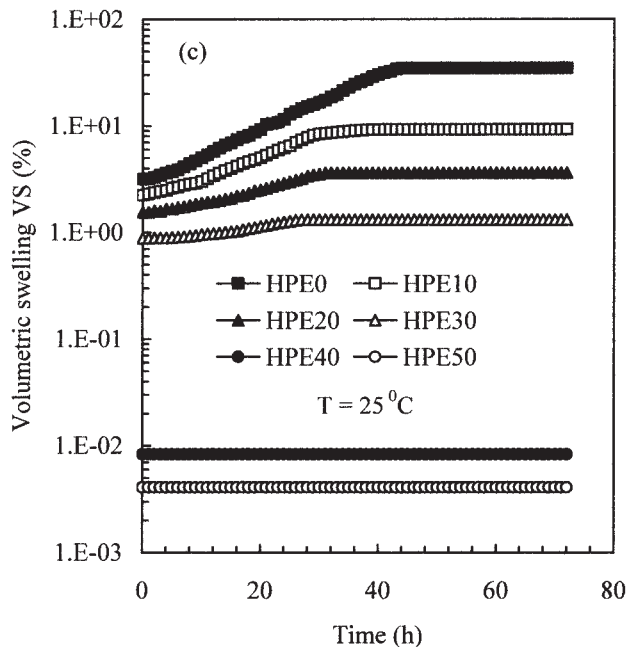
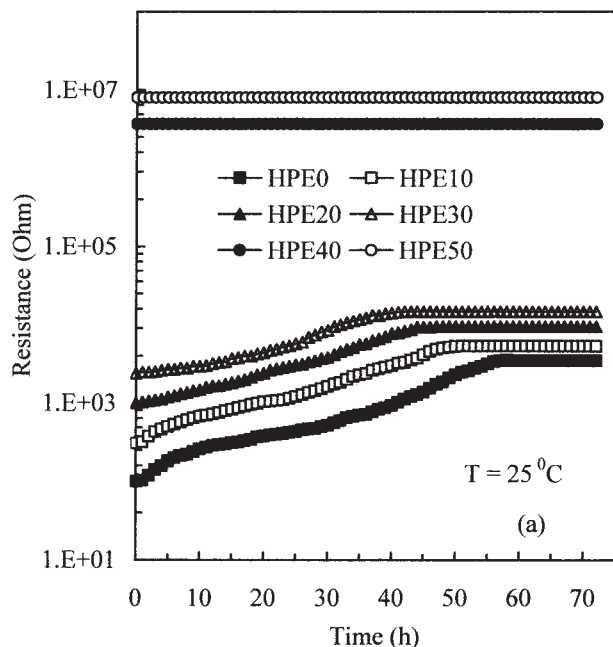


Figure 5 (a) Time dependence of the resistance of IIR/HPE blends during swelling in gasoline at 25°C, (b) E_a of the blends before and after swelling, and (c) time dependence of VS for IIR/HPE blends during swelling in gasoline at 25°C.

Figure 5(c) shows the VS curve of the IIR/HPE blends. VS decreases with increasing HPE concentration; that is, the absorbability of gasoline molecules decreases with increasing HPE concentration within the blend matrix. In other words, when the HPE concentrations are less than 30 wt %, the blend is swollen, and its VS is bigger. The chain segments of the blend are extended, and a large number of gasoline molecules penetrate the blend rapidly. The swelling rates become slower and the equilibrium swelling time becomes longer with increasing HPE concentration in the blend. With increasing HPE concentration greater than 30 wt %, the fibril-like morphology hinders the

movements of chains and the penetration of gasoline molecules into the blends. This makes VS lower and the equilibrium swelling time longer. We have concluded that the higher VS value for HPE0 than for HPE50 is due to the lower crosslinking density and interfacial adhesion of HPE0.

To understand this observation, SEM photographs of swollen IIR/HPE (0 wt % HPE loading) and IIR/HPE (50 wt % HPE loading) are plotted in Figure 6(a,b), respectively. In Figure 6(a) (i.e., swollen sample HPE0), many pores form and disperse into the rubber matrix. The presence of pores (holes) in the sample indicates a weak IIR/HPE matrix interaction. In Fig-

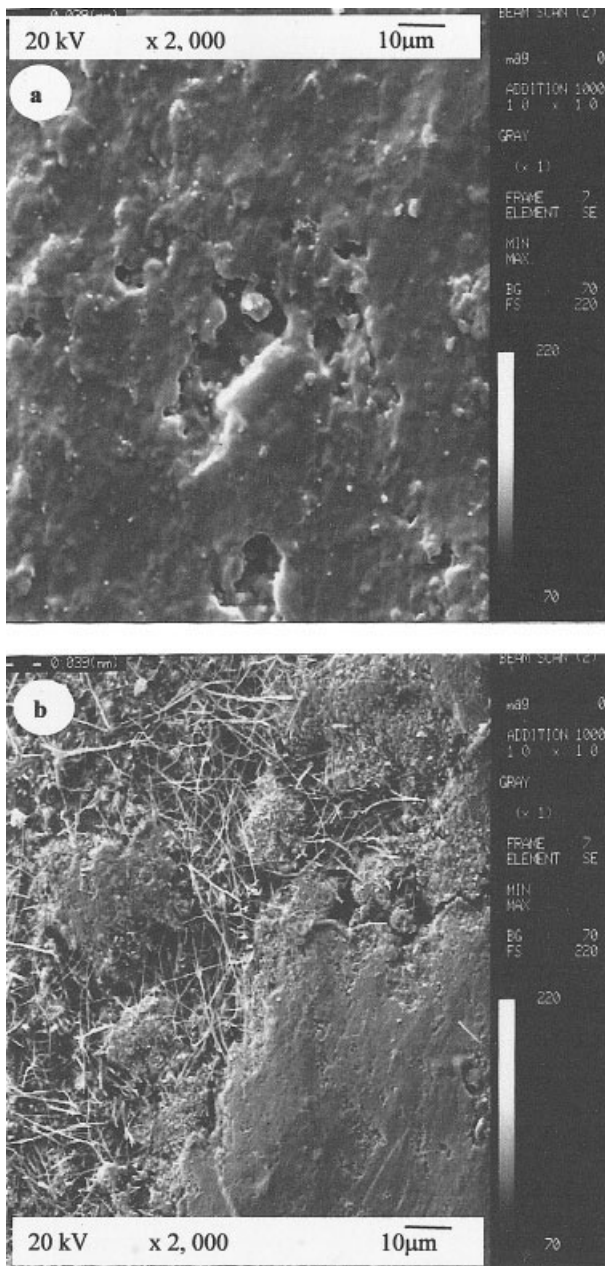


Figure 6 SEM micrographs of IIR/HPE blends (a) with an HPE loading of 0 wt % after swelling and (b) with an HPE loading of 50 wt % after swelling.

ure 7(b) (i.e., HPE50), we find that the added HPE reacts with the IIR matrix and gives a fibril-like morphology. There is no hole in the HPE50 sample. This observation shows that HPE enhances the interfacial adhesion with the blend matrix and resists the diffusion and permeation of gasoline molecules into the IIR/HPE blend, as confirmed before.

Gasoline-swelling mechanism, diffusion kinetics, and thermodynamic parameters

The following equation is used to determine the nature of the diffusion of a solvent into a rubber system:^{20,24}

$$\frac{m_t}{m_e} = Kt^n \tag{13}$$

where m_t and m_e are the increases in the sorption (mol %) at time t and at equilibrium, respectively; K is a rate constant depending on the structural characteristics of the polymer in addition to its interaction with the

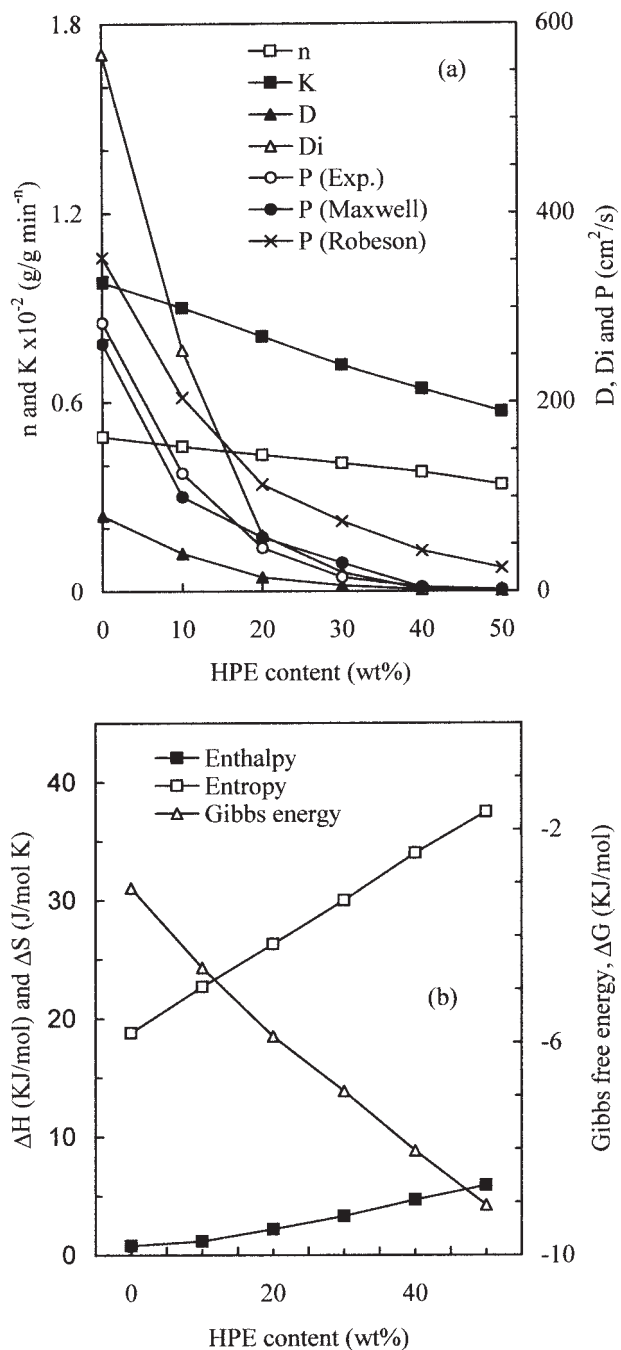


Figure 7 (a) Estimated values of K , n , D , D_i , and P as functions of the HPE concentration as well as the values of P calculated theoretically with Maxwell's and Robeson's models and (b) estimated values of ΔG , ΔS , and ΔH as functions of the HPE concentration.

gasoline solvent; and n is the diffusional exponent, which is indicative of the transport mode. When the n value equals 0.5, the swelling process is Fickian diffusion of gasoline, and this occurs when the rate of diffusion of permeant molecules is much less than the polymer segment mobility. If n is 1, the mechanism of sorption is non-Fickian diffusion, and this arises when the rate of diffusion of permeant molecules is much greater than the polymer segment mobility. If the n value lies between 1.0 and 0.5, then the mechanism of diffusion follows an anomalous trend. Then, the permeant mobility and polymer segment relaxation rates are similar.^{4,20}

According to eq. (13), a plot of $\ln(m_t/m_e)$ versus $\ln t$ should be a straight line from which the parameters K and n can be obtained. The estimated values of K and n as functions of the HPE concentration are plotted in Figure 7(a). K and n decrease with increasing HPE concentration in the rubber matrix. This indicates that the addition of HPE to the rubber matrix improves the swelling kinetics (i.e., resists the diffusion of gasoline molecules into the polymer blend). n ranges from 0.339 to 0.501, and this indicates that Fickian diffusion plays an important role in the swelling kinetics of the blends. The decrease in K with increasing HPE concentration can be attributed to effects of the crosslink structure and blend composition on the dissipation of gasoline swelling tension.²¹

However, the diffusion coefficient (D) is an important kinetic parameter of the gasoline-swelling process that indicates the transport abilities of gasoline molecules in the blend and depends on the polymer segmental mobility. From swelling data, D has been calculated as follows:

$$\frac{m_t}{m_e} = \left(\frac{4}{\sqrt{\pi}} \right) \left(\frac{Dt}{h^2} \right)^{\frac{1}{2}} \quad (14)$$

where h is the initial sample thickness.

In fact, during the diffusion process, the polymer swells, and this change in dimensions is equivalent to the occurrence of mass flow in addition to molecular diffusion. Diffusion coefficients that have been corrected for mass flow are termed intrinsic diffusion (D_i) and are given by^{4,22}

$$D_i = \frac{D}{V_r^{\frac{3}{r}}} \quad (15)$$

The values of D and D_i computed for different HPE concentrations are plotted in Figure 7(a). As could be expected, there is a decrease in the D and D_i values as the HPE concentration increases. This can be expected as at low HPE concentrations the chains are more flexible and the process of diffusion becomes much

easier. As the HPE concentration increases, the free volume decreases, and the exchange of polymer chain segments becomes less; this leads to a decrease in the values of D and D_i . The D value is optimum for the HPE0 sample. This indicates that the gasoline molecules are best accommodated in the HPE0 sample. This is because of the amorphous nature of the green IIR sample. The blends have various proportions of HPE, which is crystalline and offers resistance to the uptake of gasoline molecules, and it is more difficult to accommodate larger molecules in the polymer matrix.

The permeation coefficient (P) is a collective process of diffusion and sorption, and so the permeability of gasoline molecules into a blend sample depends on both the diffusion and solubility (S). P has been calculated with the following expression:^{4,23}

$$P = DS \quad (16)$$

S is given by

$$S = \frac{m_s}{m_p} \quad (17)$$

where m_s is the mass of the solvent taken up at equilibrium swelling and m_p is the mass of the polymer sample.

Also, P can be computed theoretically with Robeson's and Maxwell's models:²⁵

$$P(\text{Robeson}) = \frac{P_1 P_2}{\phi_1 P_2 + \phi_2 P_1} \quad (18)$$

$$P(\text{Maxwell}) = P_m \left[\frac{P_d + 2P_m - 2\phi_1(P_m - P_d)}{P_d - 2P_m + \phi_1(P_m - P_d)} \right] \quad (19)$$

where P_1 and P_2 are the permeation coefficients of HPE and IIR, respectively; ϕ_1 and ϕ_2 are the volume fractions of HPE and IIR, respectively; and the subscripts d and m correspond to the dispersed phase and the polymer matrix, respectively.

Figure 7(a) depicts the measured and theoretical values of P as a function of the HPE concentration. The P value decreases with an increase in the HPE concentration in the blends and shows the same trend as D . This means that the presence of HPE hinders the movement of gasoline molecules between the polymer segments. In addition, the decrease in P with an increase in the HPE concentration can be explained if we consider c between the solvent and polymer blend. The decreasing c values in Figure 3(a) support the observed trend in P . The experimental values of P are close to the values of Maxwell's model and far from those of Robeson's model.

However, the standard ΔS , ΔH , and ΔG values of the blends provide useful information for their suc-

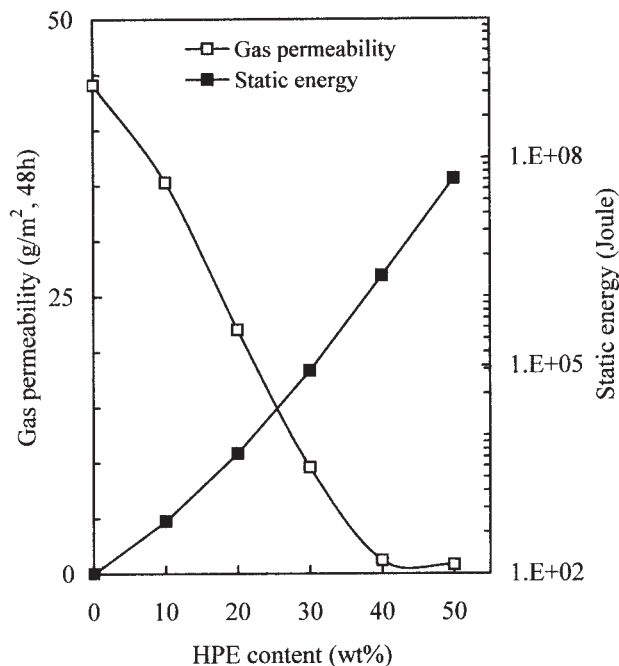


Figure 8 Dependence of the gas permeability and SE on the HPE concentration for IIR/HPE blends.

cessful applications as shielding materials. ΔS , ΔH , and ΔG of the IIR/HPE blend have been calculated with simple mathematical relations:^{4,25}

$$\Delta S = -R[\ln(1-V_r) + V_r + \frac{\rho_r V_1}{M_c} \left(\frac{V_r}{3} - \frac{V_r}{2} \right)] \quad (20)$$

$$\Delta G = RT[\ln(1-V_r) + V_r + \chi V_r^2] \quad (21)$$

$$\Delta H = \Delta G + T\Delta S \quad (22)$$

The calculated values of ΔS , ΔG , and ΔH as functions of the HPE concentration for IIR blends are plotted in Figure 8(b). ΔS , ΔG , and ΔH increase with increasing HPE concentration in the blend. This can be attributed to the fact that, with increasing HPE concentration, NEC and the interfacial adhesion increase in the blend. That ΔH and ΔS are positive values suggests that the gasoline molecules have to make room for themselves in the blend matrix and the sorption mechanism is an endothermic process. The ΔG values of all the samples are negative. This suggests that there is retention of the liquid structure in the sorbed state within the polymer matrix.

Applicability of the IIR/HPE blends as gas barriers and for antistatic charge dissipation

For successful applications of polymers as effective barriers to gases, it is important to estimate their permeability characteristics for the penetrant gas mole-

cules. Figure 8 shows the dependence of the Freon permeability on the HPE concentration for IIR/HPE blends. The addition of HPE can effectively improve the permeability of IIR/HPE blends. The permeability decreases with increasing HPE concentration in the blends. There are two main reasons for the enhancement of the Freon barrier property of the IIR/HPE blends. First, gas-impermeable HPE fibers that disperse in the rubber matrix form a tortuous channel, which retards the progress of Freon molecules through the blends. Second, the good interfacial adhesion and larger contact thickness of the blends strongly restrict the motion of the rubber chains, probably reducing the diffusivity of the Freon molecules.²⁰

SE increases with increasing HPE concentration in the blend, as shown in Figure 8. The values of SE indicate that the IIR/HPE blends at a high loading level (i.e., >30 wt % HPE) can be used for antistatic charge dissipation. Then, it can be concluded from the results of the permeability and state energy studies that the IIR/HPE blends are beneficial for Freon barriers and antistatic charge dissipation, particularly at high HPE loading levels.

Mechanical properties of the IIR/HPE blends

The use of polymer blends in industrial technologies requires a thorough knowledge of their mechanical properties. Technological processes of production can be better controlled when the relationship between the mechanical properties and the compositions of green input materials is known. The mechanical properties of a polymer depend, to a great extent, on its morphological structure.¹² Figure 9 shows the dependence of the tensile strength (TS), stiffness, hardness (H_v), and elongation at break (EB) of IIR/HPE on the HPE concentration in the matrix. Clearly, TS increases, as expected, with increasing HPE concentration. There are two possible explanations for the ability of HPE to improve TS. First, the use of HPE permits within a shorter curing time an increase in the rubber-bound and uniform dispersion of HPE in the IIR matrix, which is more beneficial for improving the plastic deformation ability of the IIR matrix. Second, HPE increases the interfacial adhesion and γ between the rubber matrix and HPE molecules. The increase in stiffness due to the addition of HPE can thus be said to be due to the formation of matrices with a much higher crosslinking density upon the incorporation of HPE.²⁵

The Shore A hardness of the blends is presented in Figure 9. The augmentation of H_v with increasing HPE concentration is mainly attributed to two factors: (1) an increase in the crosslinking density and the formation of chemical bonds between HPE and rubber chains and (2) a stronger molecular interaction between IIR and HPE molecules associated with a larger

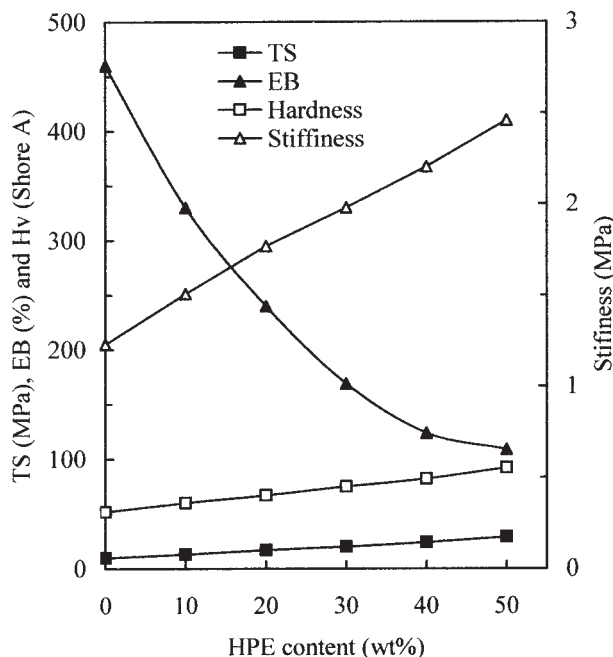


Figure 9 TS, H_v , stiffness, and EB of IIR/HPE blends.

contact area resulting in more effective constraint of the motion of rubber chains. Finally, EB of the IIR/HPE blends decreases rapidly with increasing HPE concentration. This is attributed to the fact that, with increasing HPE in the rubber matrix, the molecular motion of macromolecules is highly restricted. This leads to resistance to molecular flow and to lower resistance to break.⁴

CONCLUSIONS

We have investigated the cure characteristics, interaction parameters and chain density, swelling kinetics, diffusion mode, thermodynamic parameters, gas permeability, antistatic charge, and mechanical properties of IIR/HPE blends. The following results have been obtained.

1. The curing kinetics and molecular structure of the IIR/HPE blends improve with increasing HPE concentration. The addition of HPE reduces τ , accelerates the driving force, and increases the cure rate of the blends. HPE molecules act as bonding agents in the blend.
2. Both η and γ of the blends increase as the HPE concentration increases.
3. The morphology of the blends indicates the improvement of interfacial adhesion and contact surface between HPE and the rubber matrix.
4. The swelling kinetics and gas permeability are significantly affected by the blend composition. Zero gasoline sorption and Freon permeability

are found at higher concentrations of HPE in the blends. The mechanism of the gasoline-swelling process is controlled by Fickian diffusion in the blends.

5. D , D_{ij} and P of the gasoline in the blends decreases with increasing HPE concentration. The experimental results of P are close to those of Maxwell's model, whereas ΔS , ΔH , and ΔG increase with increasing HPE concentration in the blends. The Gibbs free energy of sorption was found to be negative for all samples, and this suggests that the sorption mechanism is an endothermic process.
6. The increase in the mechanical properties of the IIR/HPE blends is due to the large amount of plastic deformation of the rubber matrix and the increase in the interfacial adhesion of the blends.
7. Applications of this new type of IIR/HPE blend to gasoline and Freon barriers and antistatic charge dissipation with good mechanical properties have been proposed.

References

1. Harper, C. A. Handbook of Plastics, Elastomers and Composites; McGraw-Hill: New York, 1996.
2. Roland, C. M. Handbook of Elastomers New Development Technology; Marcel Dekker: New York, 1988.
3. Robeson, L. M.; Noshay, A.; Matzner, M. Angew Makromol Chem 1973, 29, 47.
4. El-Tantawy, F. Polym Degrad Stab 2001, 73, 289.
5. Chern, J. M.; Lee, W. F.; Hsieh, M. Y. J Appl Polym Sci 2004, 92, 3651.
6. Flory, P. J.; Rehner, J. J Chem Phys 1943, 11, 512.
7. Laing, Y.; Wang, Y.; Wu, Y.; Lu, Y.; Zhang, H.; Zhang, L. Polym Test 2005, 24, 12.
8. Jacob, M.; Thomas, S.; Varughese, K. T. Compos Sci Technol 2004, 64, 955.
9. Goto, S. I.; Kimura, K.; Yamashita, S. J Appl Polym Sci 1999, 74, 3548.
10. Hashim, A. S.; Ong, S. K. Polym Int 2002, 51, 611.
11. Sobhy, M. S.; Mohdy, M. M. M.; Abdel-Bary, E. M. Polym Test 1997, 16, 349.
12. Mateo, J. L.; Bosch, P.; Senano, J.; Calvo, M. Eur Polym J 2000, 36, 1803.
13. George, S. C.; Knorgen, M.; Thomas, S. J Membr Sci 1999, 163, 1.
14. Li, Y.; Zhang, Y. Polym Test 2004, 23, 83.
15. Ismail, H.; Shuhelmy, S.; Edyhom, M. R. Eur Polym J 2002, 38, 39.
16. El-Tantawy, F.; Sung, Y. K. Mater Lett 2004, 58, 154.
17. Joseph, A.; Mathai, A. E.; Thomas, S. J Membr Sci 2003, 220, 13.
18. Yan, H.; Sun, K.; Zhang, Y. Polym Test 2005, 24, 32.
19. George, S. C.; Thomas, S.; Ninan, K. N. Polymer 1996, 37, 3839.
20. Aminabhavi, T. M.; Harlapur, S. F.; Ortege, J. D. Polym Test 1997, 16, 91.
21. Unnikrishnan, G.; Thomas, S. Polymer 1998, 39, 3933.
22. Ismail, H.; Supri, M.; Yusof, A. M. M. Polym Test 2004, 23, 675.
23. Hopfenbeng, H. B.; Paul, D. R. In Polymer Blends; Paul, D. R., Ed.; Academic: New York, 1986; Vol. 1.
24. Gwaily, S. E.; Badawy, M. M.; Hassan, H. H.; Madani, M. Polym Test 2003, 22, 3.
25. Mark, J. E.; Erman, B. Rubberlike Elasticity: A Molecular Primer; Wiley: New York, 1988.